International Journal of Applied Earth Observation and Geoinformation 53 (2016) 76–89

Contents lists available at ScienceDirect

International Journal of Applied Earth Observation and Geoinformation

journal homepage: www.elsevier.com/locate/jag

Mapping *Prosopis* spp. with Landsat 8 data in arid environments: Evaluating effectiveness of different methods and temporal imagery selection for Hargeisa, Somaliland

Wai-Tim Ng[a,*], Michele Meroni[b], Markus Immitzer[a], Sebastian Böck[a], Ugo Leonardi[c], Felix Rembold[b], Hussein Gadain[c], Clement Atzberger[a]

[a] *Institute for Surveying, Remote Sensing and Land Information (IVFL), University of Natural Resources and Life Sciences, Vienna (BOKU), Peter Jordan Straße 82, 1190 Vienna, Austria*
[b] *Joint Research Center of the European Commission, MARS Unit, Via Fermi 2749, TP. 266, 21027Ispra (VA), Italy*
[c] *Food and Agriculture Organization of the United Nations, Somalia Water and Land Information Management (FAO-SWALIM) Project, P. O. Box 30470-00100 Nairobi, Kenya*

ARTICLE INFO

Article history:
Received 10 June 2016
Received in revised form 22 July 2016
Accepted 26 July 2016
Available online 17 August 2016

Keywords:
Prosopis spp.
Invasive species
Random forest classifier
OBIA

ABSTRACT

Prosopis spp. is a fast and aggressive invader threatening many arid and semi-arid areas globally. The species is native to the American dry zones and was introduced in Somaliland for dune stabilization and fuel wood production in the 1970's and 1980's. Its deep rooting system is capable of tapping into the groundwater table thereby reducing its reliance on infrequent rainfalls and near-surface water. The competitive advantage of *Prosopis* is further fuelled by the hybridization of the many introduced subspecies that made the plant capable of adapting to the new environment and replacing endemic species. This study aimed to test the mapping accuracy achievable with Landsat 8 data acquired during the wet and the dry seasons within a Random Forest (RF) classifier, using both pixel- and object-based approaches. Maps are produced for the Hargeisa area (Somaliland), where reference data was collected during the dry season of 2015. Results were assessed through a 10-fold cross-validation procedure. In our study, the highest overall accuracy (74%) was achieved when applying a pixel-based classification using a combination of the wet and dry season Earth observation data. Object-based mapping were less reliable due to the limitations in spatial resolution of the Landsat data (15–30 m) and problems in finding an appropriate segmentation scale.

1. Introduction

Prosopis spp. are an extremely drought-tolerant and widespread tree species native to American dry zones (Pasiecznik et al., 2001). In the 1970's and 1980's, a selection of different species of *Prosopis* genus were introduced in Somaliland for fuel wood production, dune stabilization after severe droughts (NAS, 1980; Von Maydell, 1986), and restoration of ecosystems degraded by war-displaced populations (Awale and Sujule, 2006). The species, hybridized and evolved in a hybrid species specifically adapted to the environmental conditions of East Africa, rendering it a superior and aggressive competitor to endemic species (Hunziker et al., 1986; Pasiecznik et al., 2001; Tessema, 2012). For simplicity, we will address hereafter all subspecies and hybrids simply as *Prosopis*.

The competitive advantage of *Prosopis* stems from several characteristics:

- extensive and deep rooting system, capable of growing tens of meters until tapping into a deep groundwater, thus reducing the dependency on rain water (Pasiecznik et al., 2001);
- vigorous production of pods high in sugar content and palatable to a variety of wild and domesticated fauna in addition to facilitated germination though animal digestion (Kipchirchi et al., 2011; Koech et al., 2010; Solbrig and Cantino, 1975);
- effective dispersal strategy characterized by combination of water and animal dispersal (Berhanu and Tesfaye, 2006; Mworia et al., 2011; Solbrig and Cantino, 1975) resulting in long distance transportation and an initial establishment along riparian zones

* Corresponding author.
E-mail address: tim.ng@boku.ac.at (W.-T. Ng).

http://dx.doi.org/10.1016/j.jag.2016.07.019
0303-2434/

Table 1
Land cover classes observed during the field campaign and used for the classification of the study area of Hargeisa. *Prosopis* is present in different degrees in classes 1–5 and absent in the eleven remaining classes. The total number of manually delineated polygons (MDP) is 332, with 48,955 pixels at 15 m resolution.

Class	Name	Description	MDP (*n*)	Pixels (*n*)
1	*Prosopis* >50%	*Prosopis* cover over 50%, such as dense thickets	26	626
2	*Prosopis* <50%	*Prosopis* cover under 50% or dry areas and soils	20	784
3	Mix >50%	*Prosopis* dominant, more than 50% cover, mixed with natural vegetation	21	603
4	Mix 25–50%	*Prosopis* sub-dominant, less than 50% cover, mixed with natural vegetation	20	1100
5	Mix <25%	*Prosopis* present, less than 25%, mixed with natural vegetation	11	729
6	Nat >50%	Natural vegetation covering more than 50%	20	1132
7	Nat 25–50%	Natural vegetation covering less than 50%	20	4681
8	Nat <25%	Natural vegetation covering less than 25%	22	11174
9	Agri irri	Irrigated agriculture	28	627
10	Agri rain	Rainfed agriculture	20	4488
11	Build up	Build up and urban areas	24	4043
12	Wadi sand	Dry river beds	20	4355
13	Rocky soil	Darker soils with rocky outcrops	20	5180
14	Dark bare soil	Dark and barren soils found at higher elevations	20	5805
15	Sandy soil	Darker sandy soils	20	2115
16	Red soil	Reddish soil found near agricultural areas	20	1513

and in proximity of human settlements typically raising livestock in the region.

For control and optimal management, *Prosopis* invasion must be first identified and regularly monitored (Shackleton et al., 2015). This is why several studies have been carried out in an effort to map the *Prosopis* invasion in Africa using remote sensing data (Hoshino et al., 2012, 2011; Mwangi and Swallow, 2005; Van Den Berg et al., 2013; Wakie et al., 2016, 2014). Van Den Berg et al. (2013) used Landsat imagery and MODIS time series to describe the current extent of *Prosopis* invasion in South Africa and its spatial dynamics, and to identify areas most susceptible to future invasion. The analysis of MODIS composites indicated that *Prosopis* reaches peak development during February and May. Landsat images matching this timeframe were selected and used for classification.

Wakie et al. (2014) used November and April MODIS Enhanced and Normalized Difference Vegetation Indices (EVI and NDVI) for Afar, Ethiopia. This matches a cold and dry period early in the dry seasons of Ethiopia. During this time, the foliage of most woody shrubs and trees remains green, while herbaceous flora, such as annual grasses and agricultural crops, senesce, creating spectral contrasts for better discrimination of woody vegetation. However, the coarse resolution data at 250 m can only depict relatively large stands.

Our study builds on this experience and follows the preliminary work of Rembold et al. (2015) in Somaliland. The authors concluded that the spread of *Prosopis* is acute and affects rivers, wadis (in Somaliland referring to ephemeral rivers, usually dry except during the rainy season) and riparian environments, as well as urban and peri-urban areas. The study utilized Landsat 8 data, reference data based on geo-tagged photos from a previous FAO field campaign (Food and Agriculture Organization of the United Nations) and applied a Maximum Likelihood Classification (MLC) using two *Prosopis* classes. Their results showed that mapping *Prosopis* is difficult because the plant (i) occurs in relatively small or narrow patches, (ii) is often mixed with natural vegetation or agriculture, and (iii) is highly polymorphous in its growth forms.

Several other studies have comparatively assessed the performances of pixel- and object-based classifications but focussed on other species (Aguirre-Gutiérrez et al., 2012; Duro et al., 2012; Gao and Mas, 2008; Immitzer et al., 2016 Wang et al., 2004; Weih and Riggan, 2010 Whiteside et al., 2011). Outcomes and conclusions vary depending on the target variable(s), study area and the spatial resolution of the data. Here we extend such comparative studies for the first time to *Prosopis* mapping using state-of-the-art remote sensing methods. We develop a classification procedure based on the Random Forest (RF) classifier (Breiman, 2001) to classify five different *Prosopis* classes with Landsat 8 data from wet and dry seasons. Specifically, we comparatively assess and discuss the accuracy of:

- pixel- and object-based image classification, and
- image acquisition time (e.g. wet vs. dry season)

with the objective to detect and map *Prosopis* in Hargeisa, Somaliland and to determine the best classification approach for the target species, thereby supporting future studies covering larger areas in East Africa. Details about the map outputs from the best performing models together with ecological interpretations of the Prosopis invasion are published in Meroni et al. (2016).

2. Material and methods

2.1. Study area

The study area (Fig. 1A) is located in western Somaliland (between 9°27′ and 9°58′ N, and 43°33′ and 44°24′ E), a self-declared state internationally recognized as an autonomous region of Somalia (Fig. 1B). The study area covers 5167 km^2 and includes the state capital Hargeisa, with 750,000 inhabitants (Demographia, 2015). A comprehensive description of the study area is provided in Meroni et al. (2016).

2.2. Data collection

2.2.1. Field work and reference dataset

The study area of Hargeisa was visited during the dry season in February 2015 and ground observations were collected for areas with different degrees of *Prosopis* infestation. Due to security and logistical issues, only selected areas could be visited in the field. An additional number of reference polygons were drawn by photointerpretation of Very High Resolution (VHR) satellite data consisting of WorldView-2 and QuickBird true colour composites made available to the Food and Agriculture Organization of the United Nations, Somalia Water and Land Information Management (FAO-SWALIM) project under the NextView license. For a large number of such polygons, photointerpretation was assisted by the use of geotagged photographs taken in the field.

- The reference data used for classification distinguishes 16 land cover classes (Table 1):
- pure *Prosopis* areas with different soil coverages (class 1–2),
- areas where *Prosopis* grows mixed with other species (class 3–5),

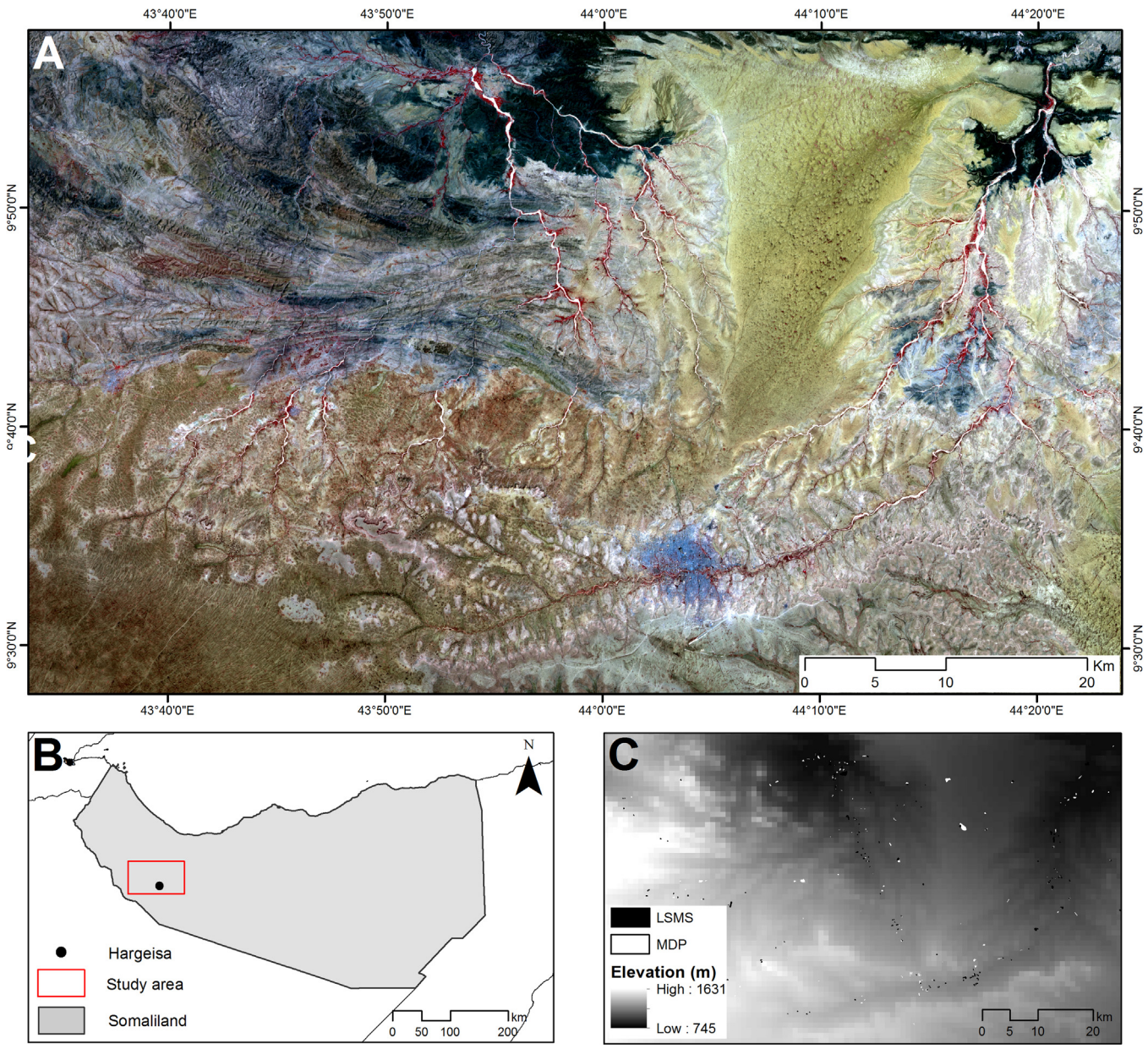

Fig. 1. (A) The study area visualized with a Landsat 8 false colour composite. (B) Outline of the study area (red box) in Somaliland (black outline) and the capital Hargeisa (dot). (C) Reference datasets visualized on Shuttle Radar Topography Mission (SRTM) (USGS, 2004) dataset. (For interpretation of the references to colour in this figure legend, the reader is referred to the web version of this article.)

- natural vegetation with different coverages (class 6–8),
- agricultural areas (class 9–10),
- build-up areas (class 11), and
- bare soils (class 12–16).

To keep the sample set relatively balanced (approx. 20–30 polygons per class), no attempts were made to regroup the (detailed) classes into fewer (broader) classes. Although increasing the overall accuracy, such a regrouping would make the samples unbalanced.

2.2.2. Satellite data and pre-processing

Two Landsat 8 Operational Land Imager (OLI) images were acquired through the USGS Earth Explorer portal and used for the mapping. One cloud free image was acquired in October (wet season) and a second image in February during the dry season (Table 2). These images were stacked and radiometrically calibrated. The datasets were compensated for different illumination conditions (sun-terrain geometry) using a 30 m resolution Digital Elevation Model (ASTER GDEM) and the C-correction method (Teillet et al., 1982). All spectral bands and the NDVI of both Landsat 8 scenes were stacked into a single raster containing fourteen bands: R, G, B, NIR, SWIR1, SWIR2 and NDVI.

Table 2
Overview of the two Landsat 8 images used in this study. All spectral channels were used, except the TIR and the coastal aerosol band.

Name	Sensor	Acquisition date	Cloud coverage
Wet season	OLI	28.10.2014	0%
Dry season	OLI	17.02.2015	0%

The original 30 m resolution was too coarse for being suitable in the object-based image analysis (OBIA). For this reason, the Landsat 8 data were pan-sharpened to 15 m resolution (Javan et al., 2013; Zhang, 2008) using the ENVI implementation of the Gram-Schmidt

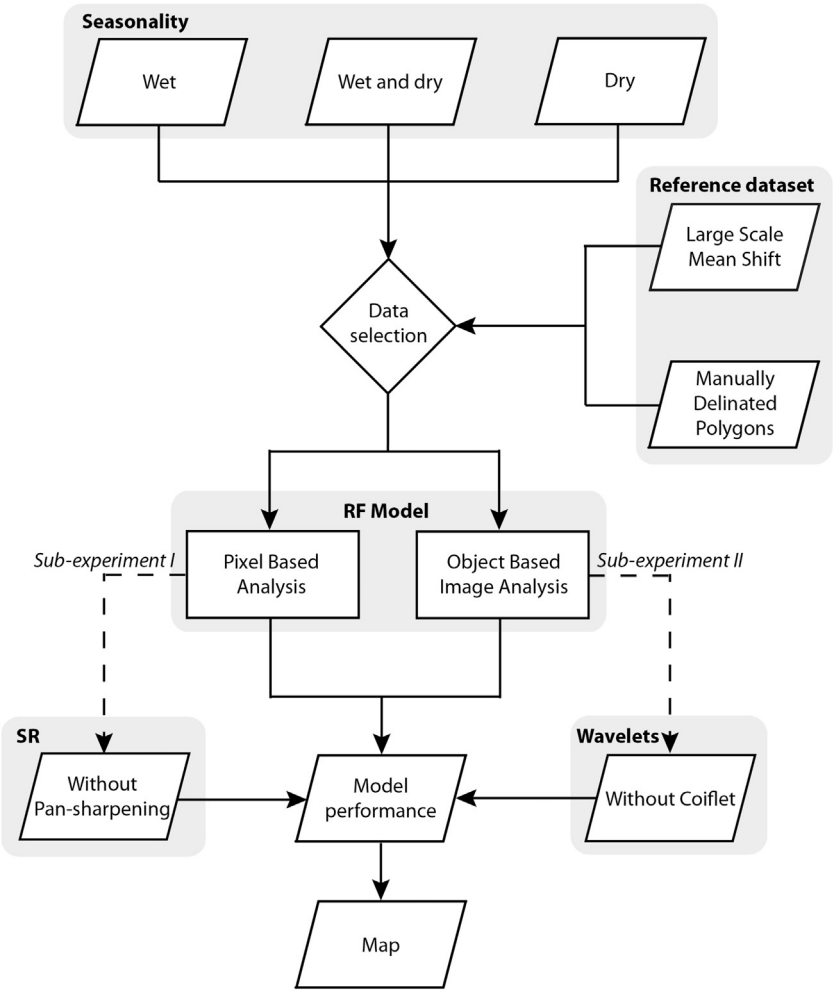

Fig. 2. General workflow of the research. We distinguish 3 × 2 combinations of seasonality of the EO input data (§2.2.2) and reference datasets (§2.2.1) using pixel- and object-based Random Forest (RF) modelling (§2.2.2). Additional sub-experiments are performed to assess the impact of wavelets (§2.2.3) (only for OBIA) and Spatial Resolution (SR) of the EO data (only for PBA) (§2.2.2).

method (Laben and Brower, 2000). Hence, the object-based mapping used only the 15 m (pan-sharpened) data, whereas datasets at 15 and 30 m were evaluated for the pixel-based approach (PBA, see sub-experiment I in Fig. 2).

2.2.3. Features used for classification

A number of studies have proven that textural features provide valuable information for OBIA applications (Du et al., 2010; Koger et al., 2003; Sakamoto et al., 2005; Toscani et al., 2013). For the purpose of our study, such features were generated based on the Coiflet wavelet transformation (Daubechies, 1992). For every spectral band we used four transformation levels and produced the mean of horizontal (H), vertical (V) and diagonal (D) detail-coefficients, by applying the Wavelet Toolbox in MATLAB 7.13.0 (MATLAB, 2012). In addition, we also calculated summary statistics per object (mean, standard deviation and percentiles), also referred to as spectral features, for each of the six spectral bands and the NDVI. Depending on which segmentation was used (see § 2.2.1), the appropriate statistics were extracted. The impact of using textural features was only assessed for the OBIA approach (see sub-experiment II in Fig. 2). No textural features were used for the pixel-based approach.

2.3. Methodology

A comprehensive overview of the implemented analysis is provided in Fig. 2. Three different Earth Observation (EO) data sets (wet, dry and combined wet and dry) are analysed with two reference data sets (Large Scale Mean Shift and Manually Delineated Polygons) to train and evaluate pixel- and object-based classifications based on RF modelling. The results are then assessed in terms of achieved accuracy. Two additional sub-experiments explore (i) the impact of wavelets on the object-based classification, and (ii) the impact of pan-sharpening of the pixel-based classification.

2.3.1. Manually delineated polygons and large scale mean shift

Two alternative reference datasets were considered. The first consists of Manually Delineated Polygons (MDP) using field information, recorded GPS coordinates, geotagged photographs taken during road trips, and photointerpretation of VHR satellite imagery and orthophotos. As a result of this process, between 20 and 30 polygons per class were digitized.

The second reference dataset was based on the Large Scale Mean Shift (LSMS) segmentation, developed by Comaniciu and Meer (2002). We used LSMS as implemented in the open source software Orfeo Toolbox version 5.0.0 (Michel et al., 2015). The LSMS algorithm was parameterized to create segments matching the MDP as much as possible, thus delineating small vegetation patches found

in the MDP. To identify the optimum segmentation parameters, five increment intervals were ran for each of the three LSMS parameters (i.e. 5^3 combinations in total): the spatial radius, the range radius and the minimum size. Before running the LSMS algorithm, the pixel values were rescaled to 8-bit values. From all the candidate segmentations, we selected an output, providing segments that most closely matched the MDPs. Optimum results were found using the following parametrization: spatial radius 15, radiometric radius 20 and minimum size 10. Finally, the class of MDPs was attributed to the overlapping LSMS segments. This resulted in approximately the same number of reference polygons per class for both reference datasets.

2.3.2. Random forest (RF) classification

We used the non-parametric Random Forest (RF) (Breiman, 2001) classifier. RF is a high performance state-of-the-art machine learning classifier based on an ensemble of decision trees. It has many benefits compared to traditional classifiers (Hastie et al., 2009; Immitzer and Atzberger, 2014; Immitzer et al., 2012; Gislason et al., 2006; Pal, 2005; Rodriguez-Galiano etal., 2012; Schultz et al., 2015):

- insensitive to the number and multi-collinearity of input data,
- no assumptions about distributions needed,
- provides information about the importance of input variables (e.g., Mean Decrease of Accuracy: MDA), and
- achieves reliable results.

In our study, all classifications were performed using the R package "RandomForest" developed by Liaw and Wiener (2002). The MDA values are used for feature ranking and selection (Genuer et al., 2010; Immitzer et al., 2012; Toscani et al., 2013; Schultz et al., 2015).

To identify the most suitable EO acquisition date and classification approach, we tested object- and pixel-based classifications with three different EO datasets (wet, dry and combined wet and dry) (Fig. 2). To make the pixel- and object-based assessments as comparable as possible, we used the same reference data set (i.e. MDP) for training and cross validation. To segment, and subsequently map, the entire study area with the object-based approach, the LSMS dataset was used, as the MDP only represent reference areas and do not cover the study areas in its entirety. This reference dataset was also assessed through a pixel-based classification.

Two additional experiments were performed to assess the impact of spatial resolution and textural features on classification accuracy. For the pixel-based classification, we investigated the performance of the (original) 30 m resolution compared to the pan-sharpened data. For the object-based classification, we used data subsets where the textural information was excluded to study the effect of wavelets on the classification accuracy. The whole processing chain was automatized developing a script in the open source statistical software R Version 3.2.3 (R Core Team, 2015).

2.3.3. Feature selection and map production using pixel- and object-based analysis

For model training and assessment of the pixel-based analysis (PBA) (Fig. 2), the MDP reference dataset based on fieldwork and photointerpretation was used. Subsequently, the model with the highest performance was identified and used to create a classified map of the study area.

The object-based analysis (Fig. 2) utilizes solely the pan-sharpened data. Similar to the pixel-based classification, three different EO datasets were evaluated. To reduce the number of input features, we performed for the two reference datasets (MDP and LSMS) a feature selection following Schultz et al. (2015). The final map was created using the best performing LSMS model with reduced feature set. Additionally, we created margin maps providing a robust measure of classification confidence derived from the underlying voting procedure (Schultz et al., 2015; Vuolo and Atzberger, 2014).

Table 3
Overview of the overall accuracy (OAA) and kappa coefficient for pixel- and object-based classifications using data collected during different periods of the year (wet, dry, combined wet and dry season). Reference data collected using manually delineated polygons (MDP) and pan-sharpened input data with ground sampling distance (GSD) of 15 m. The object-based approach includes the use of coiflet wavelets.

	Wet		Dry		Wet and dry	
Method	OAA	Kappa	OAA	Kappa	OAA	Kappa
pixel-based	70%	66%	74%	71%	73%	70%
object-based	67%	65%	75%	74%	78%	77%

2.3.4. Cross-validation

To compensate for the relatively small amount of high quality reference data for the *Prosopis* classes, we applied a 10-fold cross-validation (Kohavi, 1995). The original reference dataset was duplicated 10 times, and each time randomly split into training (90%) and validation (10%) samples. The validation dataset had always two polygons per class, corresponding to ca. 10% of the total sample size per class. A given reference polygon could be used only once for validation. By applying this rule, we generated ten unique combinations, without repetition of validation polygons.

We kept this set of combinations constant for all classifications. The omitted polygons or pixels were assessed by generating confusion matrices derived from the sum of the 10 classification results (Foody, 2002).

3. Results

A summary of pixel- and object-based classification accuracies and kappa coefficients using MDP reference is provided in Table 3 for wet, dry and combined seasons. All results refer to cross-validated experiments. Overall accuracies (OOA) show a large variability, ranging from 65% to 78% (kappa coefficient between 65% and 77%).

For both, pixel- and object-based classification approaches, better classification accuracy are achieved using EO data from the dry season compared to the wet season. The combined (wet & dry) dataset further increases the OAA for the OBIA approach. A comprehensive overview of the accuracy assessment including individual classes can be found in Appendices 1 and 2.

3.1. Pixel-based approach

The confusion matrix of PBA achieving the highest overall accuracy (73%) is shown in Table 4. Results were obtained by applying the pan-sharpened wet and dry season data at 15 m resolution on the MDP reference dataset. When evaluating individual classes, large differences in user accuracy (UA) and producer accuracy (PA) are visible. Generally, non-vegetated and agricultural classes are classified best, with UA and PA mostly in the range 70–90% (only *Rocky soils* are often miss classified as *Natural cover* <25%). High accuracies (>70%) are also found for the relatively dense and pure *Prosopis* class (*Prosopis* >50%). On the contrary, the remaining *Prosopis* classes with various coverages and/or mixtures perform significantly less well (UA and PA in the range 30–40%). Most confusion occurs between sub-classes. *Natural vegetation* classes show intermediate classification accuracies with UA and PA in the range 40–50%. A particularly high confusion is noted between *Mixed cover* <50% and *Natural cover* <50%.

Classifications using data at the original 30 m resolution degrade the results. For all cases, PBA approach using the 15 m pan-

Table 4
Confusion matrix of the pixel-based classification using pan-sharpened (15 m) wet and dry season EO data and the manually delineated polygons as reference dataset.

	Prosopis >50%	*Prosopis* <50%	Mix >50%	Mix <50%	Mix <25%	Nat > 50%	Nat <50%	Nat <25%	Agri irr	Agri rain	Build up	Wadi sand	Rocky soil	Dark bare soil	Sandy soil	Red soil	User's acc
Prosopis >50%	336	4	102	3	0	2	0	0	5	0	0	0	0	0	0	0	74%
Prosopis <50%	15	250	33	74	9	1	14	1	7	1	0	2	54	5	26	2	51%
Mix >50%	79	102	177	15	64	31	14	2	68	0	0	0	13	0	30	0	30%
Mix <50%	6	164	14	448	69	7	510	23	22	12	0	0	17	0	3	0	35%
Mix <25%	0	23	112	42	292	0	161	34	0	2	1	3	63	0	78	0	36%
Nat > 50%	28	2	26	13	0	540	440	685	4	0	0	0	47	0	0	2	30%
Nat <50%	0	26	6	386	137	376	1696	1146	34	64	0	3	35	0	0	4	43%
Nat <25%	0	2	6	62	64	48	1686	6324	0	342	8	7	676	90	451	5	65%
Agri irr	8	28	35	19	5	4	43	0	349	2	0	0	0	0	0	0	71%
Agri rain	0	0	0	12	4	0	62	150	0	4031	0	0	16	0	0	0	94%
Build up	0	7	0	0	0	0	0	33	0	0	3538	0	0	1	214	0	93%
Wadi sand	0	6	0	0	0	0	4	0	0	0	2	4339	84	0	5	0	98%
Rocky soil	0	95	32	16	43	123	41	1638	0	34	1	1	4053	1	43	41	66%
Dark bare soil	0	12	0	0	0	0	0	308	0	0	0	0	0	5708	0	0	95%
Sandy soil	0	63	20	0	8	0	0	66	0	0	40	0	54	0	1265	1	83%
Red soil	0	0	0	10	0	0	10	3	0	0	0	0	68	0	0	1458	94%
Producer's acc	71%	32%	31%	41%	42%	48%	36%	61%	71%	90%	99%	100%	78%	98%	60%	96%	73%

Table 5
Overview of the overall accuracy and kappa coefficient for pixel-based (PBA) classifications using data collected during different climatic and phenological periods of the year (wet, dry, combined wet and dry season). Reference data collected using MDP and input data with spatial resolution of 15 (pan-sharpened) and 30 m (original resolution).

	Wet		Dry		Wet and dry	
GSD	OAA	Kappa	OAA	Kappa	OAA	Kappa
15 m	70%	66%	74%	71%	73%	70%
30 m	67%	63%	70%	67%	70%	66%

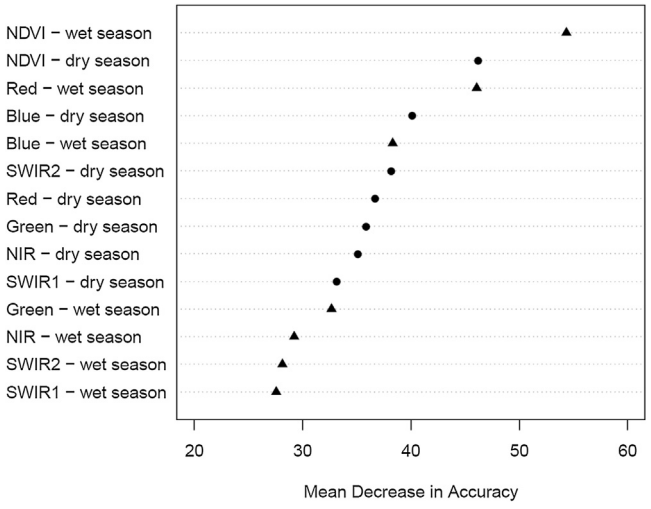

Fig. 3. MDA (Mean Decrease Accuracy) of the pixel-based classification using pan-sharpened (15 m) wet (triangle) and dry (dot) season data and MDP reference dataset.

sharpened data provides a higher overall accuracy compared to the 30 m data (Table 5). The increase in overall accuracy ranges between three and four percentage points depending on the data set used (dry, wet and combined).

The increase in accuracy with increasing spatial resolution is not equally distributed amongst classes. For all three input datasets, only the *Natural vegetation* <25% class shows a consistent increase in UA and PA when increasing the spatial resolution from 30 to 15 m (not shown). For the other classes, we observe almost no impact of spatial resolution.

The variable importance based on MDA for the combined wet and dry dataset at 15 m is shown in Fig. 3. MDA ranks the features from high (top) to low importance (bottom). The results demonstrate that the best scoring features are the NDVI (from wet season and dry season) and wet season red band showing the importance of biomass information (NDVI) and chlorophyll content (red reflectance) for class discrimination, as high NDVI and red reflectance correlate with vegetation vigour.

The four least important features are all from the wet season. From the dry season reflectances, blue, SWIR2 and red score highest, whereas green, NIR and SWIR1 have lower importance. A similar ranking is found for the spectral bands of the wet season, with the most noticeable difference that both SWIR bands score very low.

The map shown in Fig. 4 was produced using the pixel-based approach and 15 m EO data combining wet and dry season. The classification, discussed in more detail in Meroni et al. (2016), shows good agreement compared to the situation encountered in the field and reported by Rembold et al. (2015); *Prosopis* is predominantly found in urban areas (Fig. 4A) and within/along dry river beds (Fig. 4B). The drier plains and mountainous areas are absent of *Prosopis* as well as the large agricultural areas in the south-west of the study region.

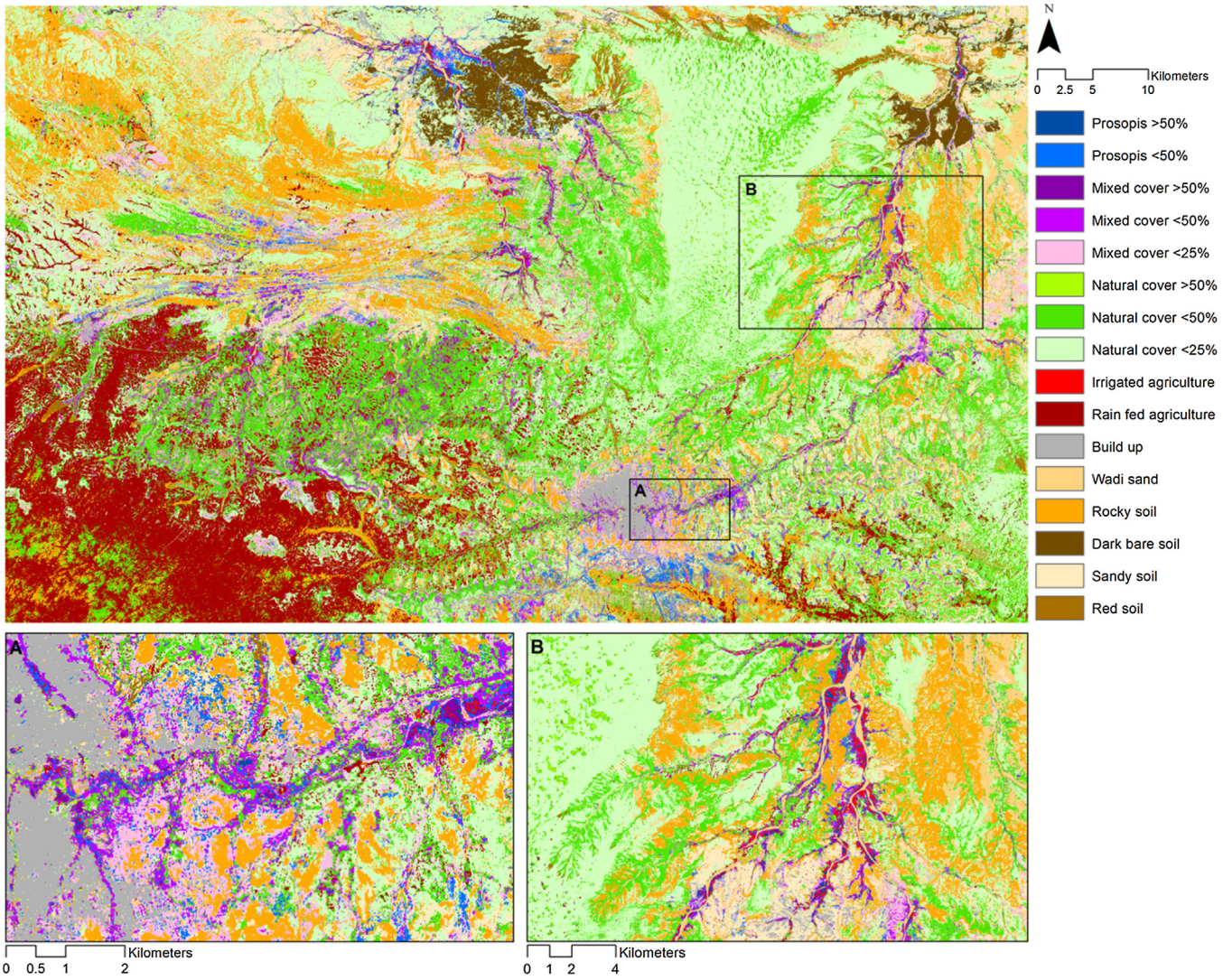

Fig. 4. Map output of the study area using a pixel-based classification and pan-sharpened wet and dry season EO data at 15 m resolution and the manually delineated polygons (MDP) as reference data set. (A) Snapshot of the *Prosopis* encroachment in the vicinity of Hargeisa. (B) *Prosopis* invasion along the dry river beds. Both situations were encountered in the field and have been described in literature.

The margin map (Fig. 5) was generated by differencing the probabilities of the first (majority vote) and second most likely assigned classes per pixel. Values range from 0 to 1 indicating low to high confidence in the attribution to the class. The map displays a high degree of uncertainty of *Light soils* and sparsely vegetated areas. High uncertainty values were also achieved for the classes *Dark soils, Wadi soils, Agriculture* and *Build up*. The *Prosopis* classes, on the other hand, received values equal to an intermediate level of classification confidence.

3.2. Object-based approach

Mapping large areas at object-level requires an automated image segmentation. For this reason, we provide separate results for the MDP and the automated LSMS segmentation. The MDP classification provides a suitable comparison with the pixel-based classification results reported in the previous section, while LSMS results are important for mapping purposes, as they cover the study area in its entirety. Object Based Image Analysis (OBIA) results for MDP and LSMS are summarized in Table 6.

3.2.1. Using the manually delineated polygons (MDP)

Compared to the pixel-based classification (Table 3), the object-based classification using MDP and EO data from wet and dry season at 15 m spatial resolution, increases the classification accuracy (Table 6). Similar to the PBA, the combined (wet and dry) input provides the highest overall accuracy (OAA of 78%); the OAA decreases compared to the pixel-based approach when only wet season data is used while a slight increase is observed for the dry data.

The confusion matrix from the best performing (wet and dry) dataset is shown in Table 7. Compared to the pixel-based classification (Table 4), the OBIA approach leads to considerably better results for several classes, e.g. for all *Prosopis* classes, *Natural vegetation* >50%, *Irrigated agriculture* and most of the *soil* classes.

Including texture information using coiflet wavelets slightly decreases (1%) the overall accuracy of the OBIA using the MDP reference dataset, except for the wet and dry season data where the OAA decreases by one percent (not shown). A positive effect of the texture measurement on the OAA was observed when performing the OBIA on the LSMS reference dataset. In this case OAA was increased by the use of textural information, regardless of the temporal dataset used by two to three percentage points.

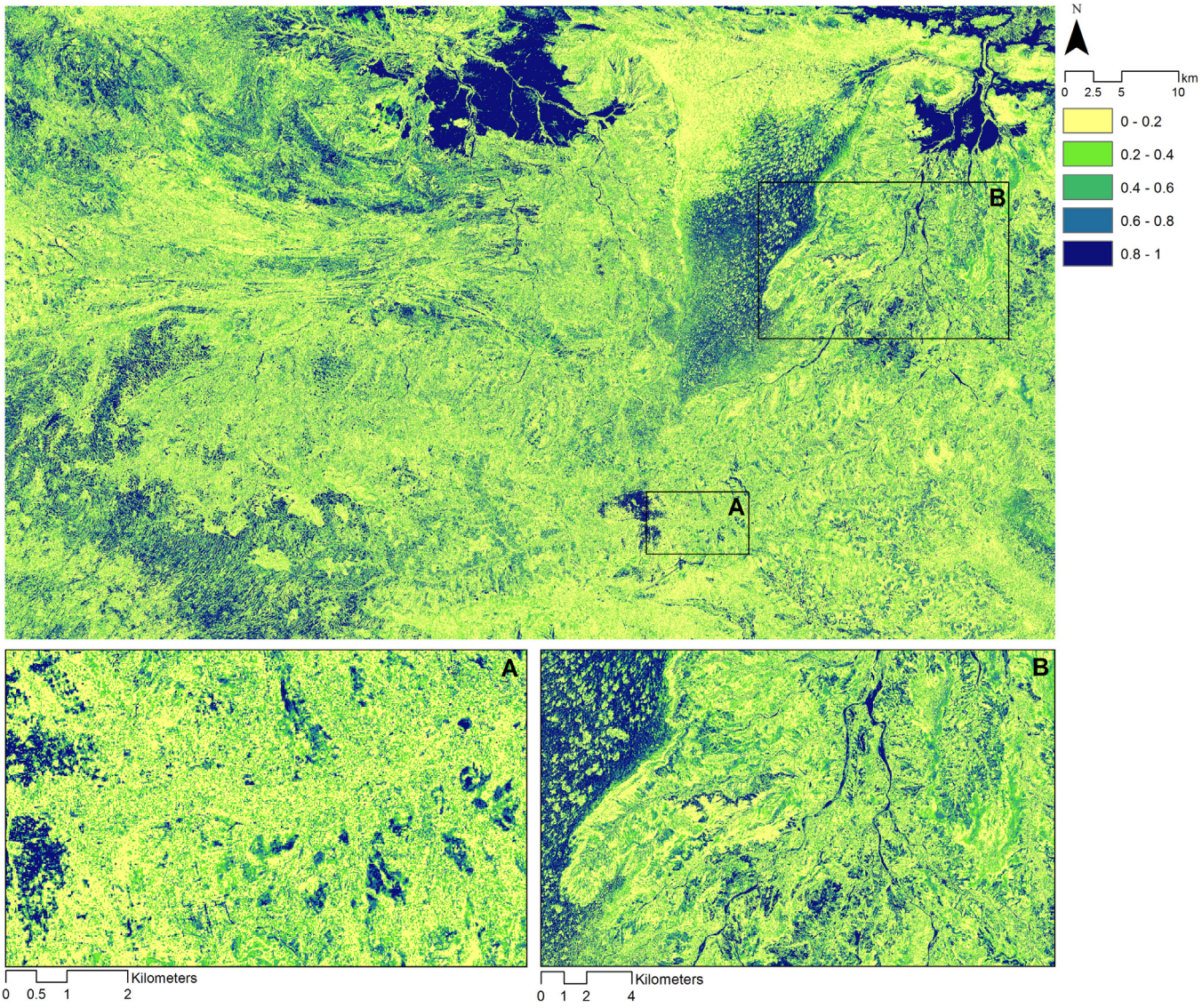

Fig. 5. Margin map for the pixel-based classification using the manually delineated polygons (MDP) as reference. The degree of confidence in the classification is expresses from 0 (low confidence) to 1 (high confidence). The area of the margin map is identical with the classification map shown in Fig. 4. (A) Detail of the Hargeisa and high confidence of the *build up* and *rocky soils* classes. (B) The dry river bed (*Wadi sand*) can be easily distinguished as high confidence areas together with the *Nat* <25% class.

Table 6
Overview of the overall accuracy (OAA) and kappa coefficient for object-based classifications using pan-sharpened data at 15 m collected during different periods of the year (wet, dry, combined wet and dry season). Reference data collected using Manually Delineated Polygons (MDP) and automated segmentation (LSMS).

		Wet		Dry		Wet and dry	
Reference	Coiflet	OAA	Kappa	OAA	Kappa	OAA	Kappa
MDP	Yes	67%	65%	75%	74%	78%	77%
MDP	No	68%	66%	76%	75%	77%	76%
LSMS	Yes	63%	60%	70%	68%	71%	69%
LSMS	No	60%	57%	68%	66%	69%	67%

3.2.2. Automated LSMS segmentation

The classification results of the OBIA using the Manually Delineated Polygons (MDP) indicate that higher accuracies can be achieved by applying an object-based approach. However, this approach cannot be used to segment large areas. To classify the entire study area, we therefore repeated the classification by substituting the MDP with the automated Large Scale Mean Shift (LSMS) segmentation. Table 8 presents the confusion matrix of the best object-based result using both wet and dry season data, recording an overall accuracy of 71%. Compared to the object-based classification using the MDP (Table 6) the overall accuracy decreases by approximately four to six percent.

The difference between MDP and LSMS amounts up to eight percent (not shown). When comparing the LSMS results to the pixel-based classification results (Table 5), the overall accuracy drops by one to seven percentage points depending on the season. Only for *Natural vegetation* <50% and <25% LSMS outperforms the pixel-based classification as well as the object-based classification using the MDP.

The MDA (Fig. 6) highlights the importance of NDVI for the classification. Six out of the top eight features refer to NDVI, with the

Table 7
Confusion matrix of the combined classification results for the object-based classification of the wet and dry season data at 15 m resolution, using the coiflet wavelets and the MDP reference data set. Values refer to number of polygons.

	Prosopis >50%	*Prosopis* <50%	Mix >50%	Mix <50%	Mix <25%	Nat > 50%	Nat <50%	Nat <25%	Agri irr	Agri rain	Build up	Wad sand	Rocky soil	Dark bare soil	Sandy soil	Red soil	User's acc
Prosopis >50%	16	0	1	0	0	1	0	0	0	0	0	0	0	0	0	0	89%
Prosopis <50%	0	7	1	2	0	0	1	0	1	0	0	0	0	0	0	0	58%
Mix >50%	4	0	15	0	0	0	0	1	0	0	0	0	0	0	0	0	75%
Mix <50%	0	3	0	14	1	0	3	0	0	0	0	0	0	0	0	0	67%
Mix <25%	0	2	0	0	6	0	0	2	0	0	0	0	1	0	0	0	55%
Nat > 50%	0	1	1	0	0	17	2	0	0	0	0	0	0	0	0	0	81%
Nat <50%	0	1	0	3	1	2	6	1	0	1	0	0	0	0	0	0	40%
Nat <25%	0	2	1	1	2	0	4	11	0	1	0	0	0	1	1	0	46%
Agri irr	0	3	1	0	0	0	0	0	19	0	0	0	0	0	0	0	83%
Agri rain	0	0	0	0	0	0	1	1	0	18	0	0	0	0	0	1	86%
Build up	0	0	0	0	0	0	0	0	0	0	20	0	0	0	1	0	95%
Wadi sand	0	0	0	0	0	0	0	0	0	0	0	20	0	0	0	0	100%
Rocky soil	0	0	0	0	0	0	0	2	0	0	0	0	17	0	0	0	89%
Dark bare soil	0	0	0	0	0	0	0	1	0	0	0	0	0	19	0	0	95%
Sandy soil	0	1	0	0	0	0	0	0	0	0	0	0	2	0	18	0	86%
Red soil	0	0	0	0	0	0	3	1	0	0	0	0	0	0	0	19	83%
Producer's acc	80%	35%	75%	70%	60%	85%	30%	55%	95%	90%	100%	100%	85%	95%	90%	95%	78%

Table 8
Confusion matrix of the best object-based method using LSMS segmentation. Inputs are wet and dry season data and coiflet wavelets from 15 m pan-sharpened EO data.

	Prosopis >50%	*Prosopis* <50%	Mix >50%	Mix <50%	Mix <25%	Nat > 50%	Nat <50%	Nat <25%	Agri irr	Agri rain	Build up	Wad sand	Rocky soil	Dark bare soil	Sandy soil	Red soil	User's acc
Prosopis >50%	16	0	3	0	1	0	0	0	1	0	0	0	0	0	0	0	76%
Prosopis <50%	0	7	1	3	1	0	0	1	2	0	0	0	0	0	0	0	47%
Mix >50%	2	2	6	3	0	3	0	0	0	0	0	1	0	0	0	0	35%
Mix <50%	2	3	2	9	3	0	3	0	0	1	0	0	0	0	0	0	39%
Mix <25%	0	1	1	0	14	0	0	1	0	0	0	0	1	0	1	0	74%
Nat > 50%	0	0	2	0	0	12	3	0	0	0	0	0	0	0	0	0	71%
Nat <50%	0	0	0	3	0	3	11	1	1	0	0	1	0	0	0	0	55%
Nat <25%	0	2	0	1	1	1	2	13	0	0	0	0	2	0	0	1	57%
Agri irr	0	2	1	1	0	0	0	1	16	0	0	1	0	0	0	0	73%
Agri rain	0	0	0	0	1	0	0	1	0	20	0	0	0	0	0	0	91%
Build up	0	0	0	0	0	0	0	0	0	0	19	0	0	0	1	0	95%
Wadi sand	0	0	2	0	1	0	1	0	0	0	0	15	1	0	1	0	71%
Rocky soil	0	0	1	0	1	1	0	2	0	0	0	0	14	0	2	0	67%
Dark bare soil	0	0	0	0	0	0	0	0	0	0	0	0	0	20	0	0	100%
Sandy soil	0	0	0	0	0	0	0	0	0	0	1	0	2	0	16	0	84%
Red soil	0	1	0	0	0	0	0	0	0	0	0	0	0	0	0	19	95%
Producer's acc	80%	39%	32%	45%	61%	60%	55%	65%	80%	95%	95%	83%	70%	100%	76%	95%	71%

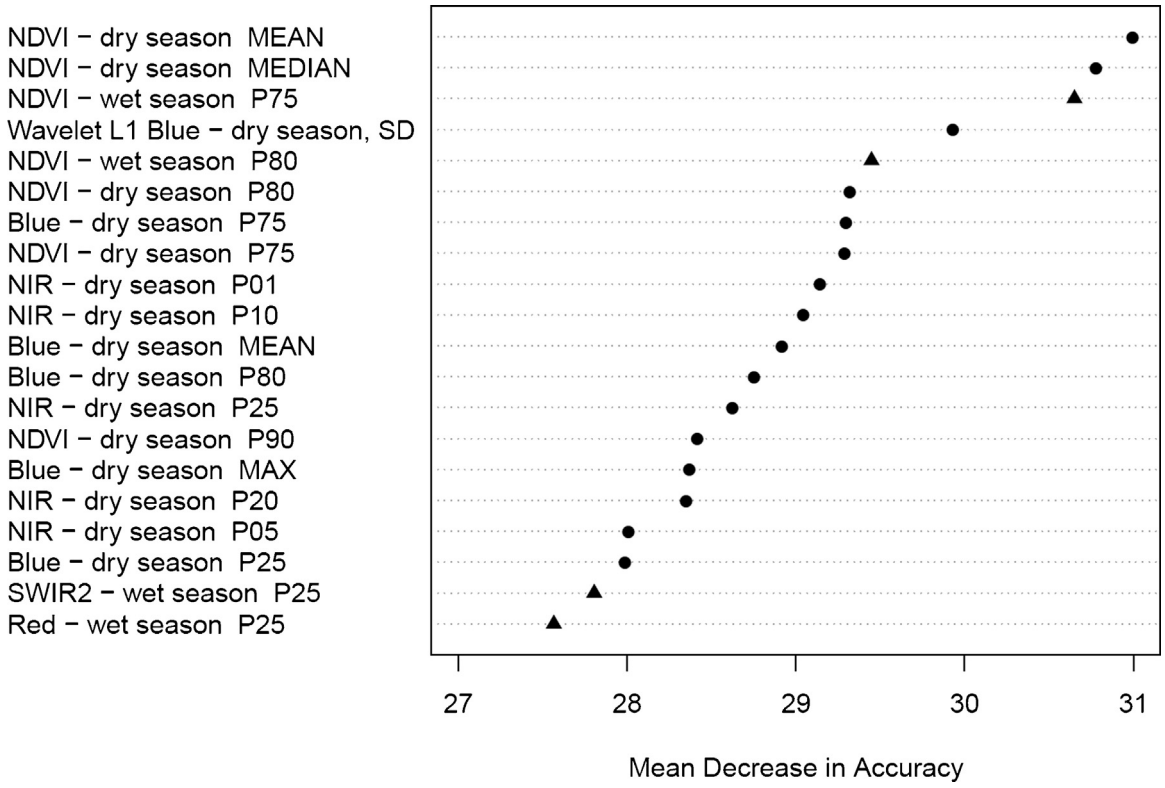

Fig. 6. MDA of the object-based classification using the LSMS reference data set on the wet and dry season data and including the coiflet wavelets.

mean of the dry season NDVI being the most important band, followed by the median of the dry season NDVI and the 75th percentile of the NDVI of the wet season. The blue band (as textural measure and 75% percentile) occurs twice in the top eight.

4. Discussion

4.1. Seasonality

Our results confirms that the timing of image acquisition has a noticeable impact on the classification accuracy (Mirik and Ansley, 2012a; Van Den Berg et al., 2013; Wakie et al., 2014). In our study, the highest overall accuracies are achieved using the combined wet and dry season data. Analysed separately, the dry season data was far more important compared to the wet season. The finding is in agreement with the known ecology of *Prosopis*. Thanks to its deep rooting system (Yoda et al., 2012) and metabolic coping system (Sen and Mehta, 1998), it remains relatively green throughout the year while endemic species (e.g. *acacia* spp.) shed their foliage during the dry season (Wakie et al., 2014). The use of the dry season image therefore increase class separability as noted by Wakie et al. (2014).

The importance of dry season data is further confirmed by the fact that the lowest class-specific accuracies for the *Prosopis* and *Mixed Prosopis* classes are found using the wet season image. Similarly, the *Irrigated agriculture* class scores notably better during the dry season. *Irrigated agriculture* is often mixed up with *Rain fed agriculture* during the wet season as irrigation-related growth differences are likely blurred.

4.2. Object- and pixel-based analysis

Our study produced an improved pixel-based *Prosopis* cover map for the Hargeisa area building on the work performed by Rembold et al. (2015) (Fig. 4) and described in more detail by Meroni et al. (2016). Looking at cross-validated results (Tables 3 and 5), we found that the highest model accuracies are achieved by performing an object-based classification using manual delineated polygons (MDP) for reference. However, this manual method can obviously not be implemented for classifying the entire study area. When substituting the MDP with the LSMS reference dataset, which covers the entire study area, the accuracy drops (the OAA from 78 to 71% using combined wet and dry data). For comparison, the pixel-based approach yields an OAA of 73% (kappa: 0.70), thus rendering the pixel-based classification the better option. The advantage of the pixel- based classification becomes even more evident, when comparing the two map products where the OBIA approach revealed stronger mis-classifications (not shown).

The reduced accuracy of the LSMS reference data set can be directly attributed to its generation. The MDP are an "optimal" reference dataset, tailored to fit each class individually, with a large variety of polygon sizes. For instance the MDP of *Prosopis* classes were typically small (i.e. from 6 to 74 pixels as 15 m) whereas the bare and sparsely vegetated areas were represented by large and homogenous polygons including hundreds of pixels (Table 1). The LSMS segmentations were generated to resemble the high quality of the MDP. However, the LSMS was unable to generate the same high quality reference polygons for all classes. As segmentation parameters cannot be class-specific, we opted for a fine scale segmentation to differentiate between the small vegetated patches. This led to an over-segmentation of the large homogeneous soil classes. As a consequence, class separability decreased compared to MDP.

Further improvements can be achieved through the method proposed by Özdemir et al., 2010, where the matching stage was implemented to find correspondences between reference (MDP) and output objects (LSMS). The authors induced a multi-object maximum overlap matching algorithm, a multi-criteria ranking procedure combining precision, recall, and detection accuracy scores, and produced a final ordering of different detection algorithms for evaluating the results.

Another consequence of the small size is the effect on the Prosopis classes, when applying the OBIA approach and the MDP. Some MDP, mainly found in the *Prosopis* and mixed classes, were too small and could not be used to extract any meaningful statistical information, used as features in the RF classifier. Thus, we opted to use only pan-sharpened data and setting a minimum segment size to 10 pixels for the LSMS segmentation, reducing quality of the training dataset.

Our findings are in line with Gao and Mas (2008) who compared pixel- and object-based classifications using Spot 5 and Landsat data resampled to 10, 30, 100 and 250 m resolution. Their results show that a decrease in spatial resolution degrades the object-based classification results. In their study, the OBIA approach outperformed the pixel-based classifications for the data sets with the highest spatial resolution.

The importance of spatial resolution data was also emphasized by Mirik and Ansley (2012b). They applied an object-based classification on both 1 and 30 m spatial resolution data for the quantification of canopy cover and infilling rates of *Prosopis glandulosa*. Their results, using four classes, show a significant increase in accuracy (OOA 93.7%, Kappa 0.89) when using 1 m aerial images compared to 30 m Landsat TM 5 data (OAA 86.9%, Kappa 0.77).

4.3. Feature importance

In our study, the feature importance ranking based on the MDA was implemented to reduce the number of features, thus minimizing over-fitting and increasing model robustness. NDVI, blue, red and SWIR bands were the most important features for the (pixel-based) classification, while for the object-based classification the NDVI is considered the most important band. This contrasts with findings of Robinson et al. (2016) that showed the effectiveness of an object-based image classification targeting *Prosopis* in Australia using very high resolution (VHR) WorldView-2 data. The study assessed WorldView-2 bands through Variable Importance in the Projection scores to identify which bands offer the highest capacity for *Prosopis* discrimination. The study reported high accuracies for *Prosopis* detection and concluded that the two near-infrared bands, followed by the red-edge and red band were the most suitable for species discrimination. As completely different sensors were used in our and Robinson's study, with different bands, band settings, acquisition dates and spatial resolutions, further research is necessary to draw resilient conclusions.

Except for the mixed *Prosopis* and *Natural vegetation* classes, the object-based classifications performed better compared to the pixel-based approaches. We argue that the object-based analysis was able to extract more information from highly heterogeneous classes, such as mixed and natural vegetation. The pixel-based approach, on the other hand, was unable to account for all the variability within the reference polygons.

In line with the results described by Toscani et al. (2013) and Koger et al. (2003), we found that the coiflet wavelets permit an increase in accuracy. Our results also show that pan-sharpening (slightly) increases the overall accuracy for the pixel-based classifications similar to the findings of Makarau et al. (2012) and Colditz et al. (2006). For the OBIA approaches, however, objects in our study were often too small for using 30 m data. Hence, only pan-sharpened data at 15 m spatial resolution was used for MDP and LSMS based classifications.

5. Conclusions

We conclude from our research, that the pixel-based approach provides the best results for the classification of *Prosopis* with Landsat 8 data. The application of wet and dry season, pan-sharpened data and the high quality manual delineated reference polygons contributed to the high classification accuracy. On the other hand, the automatically delineated reference polygons provided satisfactory results only for the reference dataset; application to the entire study area showed several shortcomings not observed using the pixel-based classification. These findings, however, do not allow to dismiss the effectiveness of the OBIA approach in general. In our study, the LSMS segmentation did not allow to capture the specific nature of *Prosopis* in Somaliland, as the spatial resolution of the Landsat 8 dataset was too coarse to resolve the patchy *Prosopis* often mixed with natural vegetation. Thus, the potential benefits of the object-based approach could not be fully exploited. We therefore recommend repeating this exercise on very high spatial resolution satellite imagery such as WorldView-3 as well as on time series of Sentinel-2 with 10 m pixel size. With spatially better resolved EO data (as compared to Landsat), we expect that the OBIA approach will show its real strengths.

Disclaimer

The authors and their respective organisations do not assume any responsibility for the geographic borders and names used for the purpose of orientation and mapping in this publication.

Acknowledgements

The Quickbird imagery was provided by the U.S. Department of State (USDS) Humanitarian Information Unit, under the NextView License.

Appendix 1 Producers's accuracy

Method	Res.	Season	Ref.	Coif.	Pj >50%	Pj <50%	Mix >50%	Mix <50%	Mix <25%	Nat > 50%	Nat <50%	Nat <25%	Agri irr	Agri rain	Build up	Wady sand	Rocky soil	Dark bare soil	Sandy soil	Red soil	Overall Acc.	Kappa
PBA	30m	wet	MDP		66%	22%	24%	20%	34%	45%	31%	49%	22%	83%	98%	95%	75%	99%	58%	92%	67%	63%
PBA	30m	dry	MDP		72%	34%	31%	35%	42%	49%	39%	49%	66%	90%	98%	100%	71%	99%	61%	93%	70%	67%
PBA	30m	w&d	MDP		68%	31%	40%	37%	48%	49%	36%	43%	72%	89%	99%	100%	77%	99%	61%	94%	70%	66%
PBA	15m	wet	MDP		68%	23%	25%	28%	28%	43%	32%	61%	18%	82%	98%	95%	75%	99%	56%	94%	70%	66%
PBA	15m	dry	MDP		71%	31%	28%	35%	48%	49%	38%	65%	62%	90%	99%	100%	74%	98%	60%	94%	74%	71%
PBA	15m	w&d	MDP		71%	32%	31%	41%	42%	48%	36%	61%	71%	90%	99%	100%	78%	98%	60%	96%	73%	70%
OBIA	15m	wet	LSMS		70%	22%	26%	25%	52%	60%	40%	50%	20%	76%	90%	83%	60%	100%	81%	95%	60%	57%
OBIA	15m	dry	LSMS		80%	28%	26%	45%	65%	60%	35%	65%	65%	90%	100%	83%	65%	100%	86%	95%	68%	66%
OBIA	15m	w&d	LSMS		70%	28%	37%	50%	70%	65%	40%	60%	65%	90%	100%	83%	70%	100%	81%	95%	69%	67%
OBIA	15m	wet	LSMS	×	70%	22%	32%	35%	70%	55%	45%	50%	40%	76%	90%	83%	60%	100%	76%	95%	63%	60%
OBIA	15m	dry	LSMS	×	80%	44%	37%	55%	57%	50%	50%	60%	65%	90%	100%	83%	70%	100%	81%	90%	70%	68%
OBIA	15m	w&d	LSMS	×	80%	39%	32%	45%	61%	60%	55%	65%	80%	95%	95%	83%	70%	100%	76%	95%	71%	69%
OBIA	15m	wet	MDP		75%	15%	70%	65%	50%	80%	15%	40%	80%	40%	95%	100%	80%	95%	80%	100%	68%	66%
OBIA	15m	dry	MDP		75%	35%	65%	65%	70%	85%	30%	60%	85%	85%	100%	100%	80%	95%	90%	95%	76%	75%
OBIA	15m	w&d	MDP		80%	30%	75%	75%	70%	85%	30%	55%	95%	85%	100%	100%	80%	95%	85%	95%	77%	76%
OBIA	15m	wet	MDP	×	75%	15%	60%	55%	60%	75%	0%	25%	80%	55%	100%	100%	75%	100%	90%	100%	67%	65%
OBIA	15m	dry	MDP	×	70%	30%	65%	70%	70%	85%	30%	55%	85%	85%	100%	100%	85%	95%	85%	95%	75%	74%
OBIA	15m	w&d	MDP	×	80%	35%	75%	70%	60%	85%	30%	55%	95%	90%	100%	100%	85%	95%	90%	95%	78%	77%

Appendix 2 User's accuracy

Method	Res.	Season	Ref.	Coif.	Pj >50%	Pj <50%	Mix >50%	Mix <50%	Mix <25%	Nat > 50%	Nat <50%	Nat <25%	Agri irr	Agri rain	Build up	Wady sand	Rocky soil	Dark bare soil	Sandy soil	Red soil	Overall Acc.	Kappa
PBA	30m	wet	MDP		68%	43%	25%	27%	30%	19%	33%	58%	31%	76%	93%	96%	66%	94%	73%	91%	67%	63%
PBA	30m	dry	MDP		72%	52%	35%	31%	41%	30%	36%	58%	59%	93%	96%	98%	62%	95%	79%	90%	70%	67%
PBA	30m	w&d	MDP		79%	56%	35%	35%	37%	21%	35%	55%	69%	94%	95%	98%	65%	94%	82%	94%	70%	66%
PBA	15m	wet	MDP		72%	36%	27%	31%	25%	29%	40%	63%	23%	77%	91%	92%	65%	95%	77%	91%	70%	66%
PBA	15m	dry	MDP		70%	48%	31%	30%	45%	37%	49%	66%	59%	92%	94%	98%	63%	95%	79%	92%	74%	71%
PBA	15m	w&d	MDP		74%	51%	30%	35%	36%	30%	43%	65%	71%	94%	93%	98%	66%	95%	83%	94%	73%	70%
OBIA	15m	wet	LSMS		64%	44%	33%	24%	44%	57%	40%	53%	25%	59%	90%	71%	63%	100%	74%	95%	60%	57%
OBIA	15m	dry	LSMS		76%	42%	33%	35%	65%	67%	39%	59%	59%	95%	95%	71%	65%	100%	90%	90%	68%	66%
OBIA	15m	w&d	LSMS		74%	42%	39%	40%	64%	68%	42%	60%	68%	95%	91%	71%	61%	100%	94%	95%	69%	67%
OBIA	15m	wet	LSMS	×	74%	57%	35%	29%	53%	50%	41%	59%	47%	73%	86%	71%	67%	100%	76%	86%	63%	60%
OBIA	15m	dry	LSMS	×	80%	47%	37%	42%	65%	67%	50%	57%	68%	86%	95%	71%	74%	100%	94%	82%	70%	68%
OBIA	15m	w&d	LSMS	×	76%	47%	35%	39%	74%	71%	55%	57%	73%	91%	95%	71%	67%	100%	84%	95%	71%	69%
OBIA	15m	wet	MDP		94%	27%	61%	50%	42%	84%	23%	42%	52%	57%	90%	95%	73%	90%	80%	95%	68%	66%
OBIA	15m	dry	MDP		83%	47%	62%	68%	58%	85%	46%	46%	68%	94%	95%	100%	80%	95%	86%	90%	76%	75%
OBIA	15m	w&d	MDP		94%	55%	71%	68%	54%	81%	43%	48%	76%	94%	95%	100%	76%	95%	89%	79%	77%	76%
OBIA	15m	wet	MDP	×	88%	30%	57%	44%	50%	75%	0%	28%	55%	73%	95%	100%	83%	91%	86%	83%	67%	65%
OBIA	15m	dry	MDP	×	93%	46%	57%	67%	50%	85%	38%	52%	65%	94%	95%	100%	81%	95%	85%	90%	75%	74%
OBIA	15m	w&d	MDP	×	89%	58%	75%	67%	55%	81%	40%	46%	83%	86%	95%	100%	89%	95%	86%	83%	78%	77%

References

Aguirre-Gutiérrez, J., Seijmonsbergen, A.C., Duivenvoorden, J.F., 2012. Optimizing land cover classification accuracy for change detection, a combined pixel-based and object-based approach in a mountainous area in Mexico. Appl. Geogr. 34, 29–37, http://dx.doi.org/10.1016/j.apgeog.2011.10.010.

Awale, A.I., Sujule, A.J., 2006. Proliferation of Honey Mesquite (Prosopis juliflora) in Somaliland: Opportunities and Challenges. Adu Dhabi, UAE.

Berhanu, A., Tesfaye, G., 2006. The Prosopis Dilemma, impacts on dryland biodiversity and some controlling methods. J. Drylands 1 (1), 158–164.

Breiman, L., 2001. Random Forests. Mach. Learn. 45, 5–32.

Colditz, R.R., Wehrmann, T., Bachmann, M., Steinnocher, K., Schmidt, M., Strunz, G., Dech, S., 2006. Influence of image fusion approaches on classification accuracy: a case study. Int. J. Remote Sens., http://dx.doi.org/10.1080/01431160600649254.

Comaniciu, D., Meer, P., 2002. Mean shift: a robust approach toward feature space analysis. IEEE Trans. Pattern Anal. Mach. 24, 603–619.

Daubechies, I., 1992. Ten lectures on wavelets. IEEE Symp. Comput. Based Med. Syst., http://dx.doi.org/10.1137/1.9781611970104.

Demographia, 2015. Demographia world urban areas & population projections. Demographia, 132.

Du, P., Tan, K., Xing, X., 2010. Wavelet SVM in Reproducing Kernel Hilbert Space for hyperspectral remote sensing image classification. Opt. Commun. 283, 4978–4984, http://dx.doi.org/10.1016/j.optcom.2010.08.009.

Duro, D.C., Franklin, S.E., Dubé, M.G., 2012. A comparison of pixel-based and object-based image analysis with selected machine learning algorithms for the classification of agricultural landscapes using SPOT-5 HRG imagery. Remote Sens. Environ. 118, 259–272, http://dx.doi.org/10.1016/j.rse.2011.11.020.

Foody, G.M., 2002. Status of land cover classification accuracy assessment. Remote Sens. Environ. 80, 185–201, http://dx.doi.org/10.1016/S0034-4257(01)00295-4.

Gao, Y., Mas, J., 2008. A comparison of the performance of pixel based and object based classifications over images with various spatial resolutions. Online J. Earth Sci. 2, 27–35.

Genuer, R., Poggi, J.-M., Tuleau-Malot, C., 2010. Variable selection using random forests. Pattern Recognit. Lett. 31, 2225–2236, http://dx.doi.org/10.1016/j.patrec.2010.03.014.

Gislason, P.O., Benediktsson, J.A., Sveinsson, J.R., 2006. Random forests for land cover classification, in: Pattern Recognition Letters. pp. 294–300. doi:10.1016/j.patrec.2005.08.011.

Hastie, T., Tibshirani, R., Friedman, J., 2009. The Elements of Statistical Learning: Data Mining, Inference and Prediction. Springer, New York, NY, USA.

Hoshino, B., Yonemori, M., Manayeva, K., Karamalla, A., Yoda, K., Suliman, M., Elgamri, M., Nawata, H., Mori, Y., Yabuki, S., Aida, S., 2011. Remote sensing methods for the evaluation of the mesquite tree (Prosopis juliflora) environmental adaptation to semi-arid Africa. Inte. Geosci. Remote Sens. Symp. (IGARSS), 1910–1913, http://dx.doi.org/10.1109/IGARSS.2011.6049498.

Hoshino, B., Karamalla, A., Abd Ebasit, M.A.M., Manayeva, K., Yoda, K., Suliman, M., Elgamri, M., Nawata, H., Yasuda, H., 2012. Evaluating the invasion strategic of mesquite (Prosopis juliflora) in eastern Sudan using remotely sensed technique. J. Arid L. Stud. 4, 1–4.

Hunziker, J.H., Saidman, B.O., Naranjo, C.A., Palacios, R.A., Poggio, L., Burghardt, A.D., 1986. Hybridization and genetic variation of Argentine species of Prosopis. For. Ecol. Manage. 16, 301–315, http://dx.doi.org/10.1016/0378-1127(86)90030-7.

Immitzer, M., Atzberger, C., 2014. Early detection of bark beetle infestation in Norway spruce (Picea abies: L.) using WorldView-2 Data. Photogramm. Fernerkundung Geoinf. 5, 351–367.

Immitzer, M., Atzberger, C., Koukal, T., 2012. Tree species classification with random forest using very high spatial resolution 8-band worldview-2 satellite data. Remote Sens. 4, 2661–2693, http://dx.doi.org/10.3390/rs4092661.

Immitzer, M., Vuolo, F., Atzberger, C., 2016. First experience with sentinel-2 data for crop and tree species classifications in central europe. Remote Sens. 8, 166, http://dx.doi.org/10.3390/rs8030166.

Javan, F.D., Samadzadegan, F., Reinartz, P., 2013. Spatial quality assessment of pan-sharpened high resolution satellite imagery based on an automatically estimated edge based metric. Remote Sens. 5, 6539–6559, http://dx.doi.org/10.3390/rs5126539.

Kipchirchi, K.O., Ngugi, K.R., Wahome, R.G., 2011. Use of dry land tree species (Prosopis juliflora) seed pods as supplement feed for goats in the arid and semi arid lands of Kenya. Environ. Res. J., http://dx.doi.org/10.3923/erj.2011.66.73.

Koech, O.K., Kinuthia, R.N., Wahome, R.G., Choge, S.K., 2010. Effects of Prosopis juliflora seedpod meal supplement on weight gain of weaner galla goats in Kenya itle. Res. J. Anim. Sci. 4, 58–62.

Koger, C.H., Bruce, L.M., Shaw, D.R., Reddy, K.N., 2003. Wavelet analysis of hyperspectral reflectance data for detecting pitted morningglory (Ipomoea lacunosa) in soybean (Glycine max). Remote Sens. Environ. 86, 108–119, http://dx.doi.org/10.1016/S0034-4257(03)00071-3.

Kohavi, R., 1995. A study of cross-validation and bootstrap for accuracy estimation and model selection. Int. Jt. Conf. Artif. Intell. 14, 1137–1143, http://dx.doi.org/10.1067/mod.2000.109031.

Laben, C., Brower, B., 2000. Process for enhancing the spatial resolution of multispectral imagery using pan-sharpening. United States Pat 6 11, 875.

Liaw, A., Wiener, M., 2002. Classification and Regression by randomForest. R. News 2, 18–22, http://dx.doi.org/10.1177/154405910408300516.

MATLAB, 2012. MATLAB and Wavelet Toolbox R. The MathWorks, Inc., Natick, Massachusetts, United States.

Makarau, A., Palubinskas, G., Reinartz, P., 2012. Analysis and selection of pan-sharpening assessment measures. J. Appl. Remote Sens. 6, 63541–63548, http://dx.doi.org/10.1117/1.jrs.6.063548.

Meroni, M., Ng, W., Rembold, F., Leonardi, U., Atzberger, C., Gadain, H., Shaiye, M., 2016. Mapping Prosopis juliflora in west Somaliland with Landsat 8 satellite imagery and ground information. L. Degrad. Dev. (in print).

Michel, J., Youssefi, D., Grizonnet, M., 2015. Stable mean-shift algorithm and its application to the segmentation of arbitrarily large remote sensing images. IEEE Trans. Geosci. Remote Sens. 53, 952–964, http://dx.doi.org/10.1109/TGRS.2014.2330857.

Mirik, M., Ansley, R.J., 2012a. Comparison of ground-Measured and image-Classified mesquite (Prosopis glandulosa) canopy cover. Rangel. Ecol. Manag. 65, 85–95, http://dx.doi.org/10.2111/REM-D-11-00073.1.

Mirik, M., Ansley, R.J., 2012b. Utility of satellite and aerial images for quantification of canopy cover and infilling rates of the invasive woody species honey mesquite (Prosopis glandulosa) on rangeland. Remote Sens. 4, 1947–1962, http://dx.doi.org/10.3390/rs4071947.

Mwangi, E., Swallow, B., 2005. Invasion of Prosopis juliflora and local livelihoods. World Agrofor. Cent. 66, http://dx.doi.org/10.4103/0972-4923.49207.

Mworia, J.K., Kinyamario, J.I., Omari, J.K., Wambue, J.K., 2011. Patterns of seed dispersal and establishment of the invader Prosopis juliflora in the upper floodplain of Tana River, Kenya. Afr. J. Range Forage Sci. 28, 35–41.

NAS, 1980. Firewood Crops: Shrub and Tree Species for Energy Production. Natl. Acad. Press, Washingt. D.C., USA, 1.

Özdemir, B., Aksoy, S., Eckert, S., Pesaresi, M., Ehrlich, D., 2010. Performance measures for object detection evaluation. Pattern Recognit. Lett. 31, 1128–1137, http://dx.doi.org/10.1016/j.patrec.2009.10.016.

Pal, M., 2005. Random forest classifier for remote sensing classification. Int. J. Remote Sens. 26, 217–222. doi: 10.1080/01431160412331269698.

Pasiecznik, N., Felker, P., Cadoret, K., Harsh, L.N., Cruz, G., Tewari, J.C., Maldonado, L.J., 2001. The Prosopis juliflora—Prosopis pallida complex: the Prosopis juliflora—Prosopis pallida complex. Managing 231, 162, http://dx.doi.org/10.1007/s00709-007-0258-7.

R Core Team, 2015. R: A Language and Environment for Statistical Computing. R Found. Stat. Comput., Vienna Austria, http://dx.doi.org/10.1038/sj.hdy.6800737.

Rembold, F., Leonardi, U., Ng, W., Gadain, H., Meroni, M., 2015. Mapping areas invaded by Prosopis juliflora in Somaliland with Landsat 8 imagery. Proc. SPIE 9637, 1–12, http://dx.doi.org/10.1117/12.2193133.

Robinson, T.P., Wardell-Johnson, G.W., Pracilio, G., Brown, C., Corner, R., van Klinken, R.D., 2016. Testing the discrimination and detection limits of WorldView-2 imagery on a challenging invasive plant target. Int. J. Appl. Earth Obs. Geoinf. 44, 23–30, http://dx.doi.org/10.1016/j.jag.2015.07.004.

Rodriguez-Galiano, V.F., Chica-Olmo, M., Abarca-Hernandez, F., Atkinson, P.M., Jeganathan, C., 2012. Random Forest classification of Mediterranean land cover using multi-seasonal imagery and multi-seasonal texture. Remote Sens. Environ. 121, 93–107. doi:10.1016/j.rse.2011.12.003.

Sakamoto, T., Yokozawa, M., Toritani, H., Shibayama, M., Ishitsuka, N., Ohno, H., 2005. A crop phenology detection method using time-series MODIS data. Remote Sens. Environ. 96, 366–374, http://dx.doi.org/10.1016/j.rse.2005.03.008.

Schultz, B., Immitzer, M., Formaggio, A.R., Sanches, I.D.A., Luiz, A.J.B., Atzberger, C., 2015. Self-guided segmentation and classification of multi-temporal Landsat 8 images for crop type mapping in Southeastern Brazil. Remote Sens. 7, 14482–14508, http://dx.doi.org/10.3390/rs71114482.

Sen, D.N., Mehta, M., 1998. Seasonal variations of metabolic status of Prosopis juliflora. Ecol. Lab. Bot. Dep. J.N.V. Univ., Jodhpur 342001, India, pp. 35–37.

Shackleton, R.T., Le Maitre, D.C., Van Wilgen, B.W., Richardson, D.M., 2015. The impact of invasive alien Prosopis species (mesquite) on native plants in different environments in South Africa. South Afr. J. Bot. 97, 25–31, http://dx.doi.org/10.1016/j.sajb.2014.12.008.

Solbrig, O.T., Cantino, P.D., 1975. Reproductive adaptations in Prosopis. J. Arnold Arbor. 56, 185–210.

Teillet, P.M., Guindon, B., Goodenough, D.G., 1982. On the slope-aspect correction of multispectral scanner data. Can. J. Remote Sens. 8, 84–106, http://dx.doi.org/10.1080/07038992.1982.10855028.

Tessema, Y., 2012. Ecological and economic dimensions of the paradoxical invasive species-Prosopis juliflora and policy challenges in Ethiopia. J. Econ. Sustain. Dev. 3, 62–71.

Toscani, P., Immitzer, M., Atzberger, C., 2013. Wavelet-based texture measures for object-based classification of aerial images. Photogramm. Fernerkundung Geoinf. 2013, 105–121, http://dx.doi.org/10.1127/1432-8364/2013/0162.

USGS, 2004. Shuttle radar topography mission. Glob. L. Cover Facil Univ., Maryland, Coll. Park. Maryland, Febr. 2000.

Van Den Berg, E.C., Kotze, I., Beukes, H., 2013. Detection, quantification and monitoring Prosopis spp. in the Northern Cape Province of South Africa using Remote Sensing and GIS 2, 1–151.

Von Maydell, H.J., 1986. Trees and Shrubs of the Sahel—Their Characteristics and Uses. Title. GTZ, Eschborn, Ger.

Vuolo, F., Atzberger, C., 2014. Improving land cover maps in areas of disagreement of existing products using NDVI time series of MODIS —example for Europe. Photogramm. Fernerkundung Geoinf. 201, 393–407.

Wakie, T.T., Evangelista, P.H., Jarnevich, C.S., Laituri, M., 2014. Mapping current and potential distribution of non-native Prosopis juliflora in the afar region of Ethiopia. PLoS One 9, e112854, http://dx.doi.org/10.1371/journal.pone.0112854.

Wakie, T.T., Laituri, M., Evangelista, P.H., 2016. Assessing the distribution and impacts of Prosopis juliflora through participatory approaches. Appl. Geogr. 66, 132–143, http://dx.doi.org/10.1016/j.apgeog.2015.11.017.

Wang, L., Sousa, W.P., Gong, P., 2004. Integration of object-based and pixel-based classification for mapping mangroves with IKONOS imagery. Int. J. Remote Sens. 25, 5655–5668, http://dx.doi.org/10.1080/014311602331291215.

Weih, R.C., Riggan, N.D., 2010. Object-based classification vs. pixel-based classification: comparitive importance of multi-resolution imagery. Int. Arch. Photogramm Remote Sens. Spat. Inf. Sci. XXXVIII, 1–6.

Whiteside, T.G., Boggs, G.S., Maier, S.W., 2011. Comparing object-based and pixel-based classifications for mapping savannas. Int. J. Appl. Earth Obs. Geoinf. 13, 884–893, http://dx.doi.org/10.1016/j.jag.2011.06.008.

Yoda, K., Elbasit, M.A., Hoshino, B., Nawata, H., Yasuda, H., 2012. Root system development of Prosopis seedlings under different soil moisture conditions. J. Arid L. Stud. 16, 13–16.

Zhang, Y., 2008. Pan-sharpening for improved information extraction. Advances in Photogrammetry Remote Sensing and Spatial Information Sciences: 2008 ISPRS Congress Book, 185–204.